THE JOURNAL OF BIOLOGICAL CHEMISTRY VOL. 286, NO. 38, pp. 33345–33357, September 23, 2011

Zebrafish *mll* Gene Is Essential for Hematopoiesis[S]

Received for publication, April 20, 2011, and in revised form, July 20, 2011 Published, JBC Papers in Press, July 22, 2011, DOI 10.1074/jbc.M111.253252

Xiaoyang Wan, Bo Hu, Jing-xia Liu, Xi Feng, and Wuhan Xiao[1]

From the Key Laboratory of Aquatic Biodiversity and Conservation, Institute of Hydrobiology, Chinese Academy of Sciences, Wuhan 430072, China

Studies implicate an important role for the mixed lineage leukemia (*Mll*) gene in hematopoiesis, mainly through maintaining *Hox* gene expression. However, the mechanisms underlying *Mll*-mediated hematopoiesis during embryogenesis remain largely unclear. Here, we investigate the role of *mll* during zebrafish embryogenesis, particularly hematopoiesis. *Mll* depletion caused severe defects in hematopoiesis as indicated by a lack of blood flow and mature blood cells as well as a significant reduction in expression of hematopoietic progenitor and mature blood cell markers. Furthermore, *mll* depletion prevented the differentiation of hematopoietic progenitors. In addition, we identified the N-terminal mini-peptide of Mll that acted as a dominant negative form to disrupt normal function of *mll* during embryogenesis. As expected, *mll* knockdown altered the expression of a subset of *Hox* genes. However, overexpression of these down-regulated *Hox* genes only partially rescued the blood deficiency, suggesting that *mll* may target additional genes to regulate hematopoiesis. In the *mll* morphants, microarray analysis revealed a dramatic up-regulation of *gadd45αa*. Multiple assays indicate that *mll* inhibited *gadd45αa* expression and that overexpression of *gadd45αa* mRNA led to a phenotype similar to the one seen in the *mll* morphants. Taken together, these findings demonstrate that zebrafish *mll* plays essential roles in hematopoiesis and that *gadd45αa* may serve as a potential downstream target for mediating the function of *mll* in hematopoiesis.

The mixed lineage leukemia (*MLL*) gene, a human homolog of *Drosophila melanogaster* Trithorax (*Trx*), was originally identified through its involvement in in-frame reciprocal translocations with partner genes primarily associated with leukemias (1–5). To date, over 70 different partner genes have been identified (6–8). The *MLL* gene encodes a 430-kDa protein containing three AT hook motifs, two speckled nuclear localization domains (SNL1 and SNL2), a C*XXC* zinc finger motif, multiple plant homology domains (PHDs),[2] and a Su/var, Enhancer or zeste, Trithorax (SET), domain. The PHD fingers contribute to protein-protein interactions, and their deletion, as a result of chromosomal translocation, is necessary for MLL fusion proteins to induce hematopoietic cell immortalization (9). The SET domain contributes to modulation of homeobox (*HOX*) gene expression by facilitating histone H3 Lys-4 methylation at the proximal promoter region (10). Recent studies have also shown that genotoxic stress induces the ATR phosphorylation of MLL, leading to increased histone H3 Lys-4 methylation and subsequent execution of the mammalian S-phase checkpoint (11). The MLL protein normally is cleaved into a specific 320-kDa N-terminal (MLL^N) and a 180-kDa C-terminal (MLL^C) fragment (12, 13). *In vivo*, wild-type MLL^N and MLL^C associate with each other as well as with other factors, such as Menin, WDR5, ASH1/2, HCF2, RBBP5, and MOF (males absent on the first), to form a large nuclear complex involved in chromatin remodeling (14–16).

The function of *Mll in vivo* has been extensively analyzed in mouse models. *Mll* heterozygous knock-out mice exhibit growth retardation, hematopoietic defects, and skeletal malformation (17). Insertion of stop codons within exon 3 or exons 12–14 of *Mll* produce a defect in fetal liver hematopoiesis and are embryonic lethal at E10.5 and E11.5–14.5, respectively (18). In addition, truncation of *Mll* at exon 5 results in early embryonic death due to failure of preimplantation (19). Chimeric mice expressing *lacZ,* but not a Myc tag, in exon 8 of *Mll* develop acute leukemias (20). However, mice that express MLL with a deleted SET domain (MLLΔSET) are viable and fertile (21). Recently, another study demonstrated an essential role for MLL in neurogenesis (22). Thus, the proper formation of an MLL super complex and functions outside of the SET domain are required for early embryonic development and organogenesis.

Although the phenotypes in *Mll* knock-out mice vary depending on the particular allele knocked out and the tissues in which *Mll* was deleted, mouse models have conclusively shown that *Mll* has an essential role in controlling *Hox* gene expression (17, 19–20, 23, 24). *Mll*-null mice initiate the expression of stage-specific *Hox* genes appropriately but do not maintain expression past embryonic day 9.5 (25). *Hox* genes, as transcription factors, participate in the development of multiple tissues, including the hematopoietic system, by conferring positional identities to cells along the anteroposterior axis (26–29). Moreover, *Mll* is required for definitive hematopoietic expansion in a *Hox*-dependent manner and is essential for the maintenance of adult hematopoietic stem cell quiescence and promoting proliferation of the progenitors (28, 31). *Mll* also plays an important role in fetal and adult hematopoietic stem cell self-renewal (32). Not surprisingly, heterozygous mice ($Mll^{+/-}$) exhibit hematopoietic abnormalities along with

[S] The on-line version of this article (available at http://www.jbc.org) contains supplemental Tables 1 and 2 and Figs. 1–7.

[1] Supported by "973" Grants 2010CB126306 and 2007CB815705, National Science Foundation of China Grants 30971667, 31071212, 91019008, and 20890113, and National Transgene Project Grant 2009ZX08010-021B. To whom correspondence should be addressed: Institute of Hydrobiology, Chinese Academy of Sciences, Wuhan 430072, China. Fax: 86-27-68780087; E-mail: w-xiao@ihb.ac.cn.

[2] The abbreviations used are: PHD, plant homology domain; MO, morpholino; hpf, hours post-fertilization; dpf, days post-fertilization; SET, Su/var, Enhancer or zeste, Trithorax.

altered *Hox* gene expression (17). Detailed assessment of yolk sac and fetal liver hematopoiesis demonstrated deficiencies in proliferation and/or survival of *Mll* null hematopoietic progenitors and delays in onset of differentiation instead of blocking specific lineages (23). Collectively, these findings provide clear evidence indicating that MLL plays a critical role in hematopoiesis, in part by regulating *Hox* gene expression.

Despite these advances in understanding the role of *Mll* in hematopoiesis, it remains unclear how *Mll*-mediated hematopoiesis occurs during embryogenesis due to the early embryonic death of *Mll*-null mice. In this study, we used morpholinos to study the function of zebrafish *mll* in hematopoiesis during embryogenesis, and we found that *mll* plays an essential role in both zebrafish primitive and definitive hematopoiesis.

EXPERIMENTAL PROCEDURES

Maintenance of Fish Stocks and Embryo Collection—For wild-type zebrafish (*Danio rerio*) (strain AB), *flk1*-GFP transgenic zebrafish (provided by Jianfang Gui, originally obtained from Shuo Lin) maintenance, breeding, and staging were performed as described previously (33).

Whole Mount in Situ Hybridization and o-Dianisidine Staining—Probes for detecting zebrafish *mll, gata1, scl, lmo2, pu.1, runx1,* c-*myb, mpo, l-plastin, hbbe1, hoxb4a, hoxb5a, hoxb7a, hoxa9a, hoxb6b, hoxc8, hoxd3a*, *cdx4,* and *gadd45αa* were PCR-amplified from zebrafish cDNA pools and subcloned into the pTA2 vector (Toyobo, Osaka, Japan). Probes for *flk* (34), *pax2a* (35), *myoD* and *nkx2.5* (36), *eph2a* (37), and *gadd45αb* (38) were described previously. All primers are listed in supplemental Table 1. The procedures for whole mount *in situ* hybridization and *o*-dianisidine staining were performed as described previously (39).

Mll Antisense Morpholinos and Their Validations—We designed a morpholino (MO) that targeted the ATG codon of *mll* to block translation (*mll*-MO1), TGCGCCATTTTACACTCTGCCTGCC. We also designed an MO that targets the exon1-intron1 splicing junction site of *mll* (*mll*-MO2), TTTAGCCAGGGTCCCGCTTACCTCC, and an MO that targets the 5′-UTR region of *mll* (*mll*-MO3), ACACTCTGCCTGCCTGCCCTAGGAT. The morpholinos were generated at Gene Tools, LLC (Philomath, OR).

For *mll*-MO1 validation, the zebrafish *mll* cDNA fragment that encompassed part of the 5′-UTR (5′-ggcaggcagagttgaaa-3′) and 252-bp fragment (246 bp of exon1 plus 6 bp of exon2) was cloned into pAcGFP-N1 (Clontech) to generate a wild-type *mll* (exon1)-GFP fusion protein expression vector (WT1). A mutated *mll* (exon1)-GFP fusion protein expression vector (MT1) was generated by PCR using a forward primer with seven mismatched nucleotides as follows: 5′-**cgg**ag**c**ca**c**a**ca**gt**t**aa-3′ (seven mismatched nucleotides are underlined).

For *mll*-MO2 validation, three primers were designed. The sequence of the primer in exon1 (P1) was 5′-ctccttatcagcgcgggaacaaat-3′; the sequence of the primer in exon2 (P3) was 5′-gggctatgtagtcttctgttgtcact-3′; and the sequence of the primer in intron1 (P2) was 5′-agacaacaacaaccaactggcacc-3′.

For mll-MO3 validation, zebrafish *mll* cDNA fragment that encompassed part of the 5′-UTR (5′-atcctagggcaggcaggcagagtgtaaa-3′) and 252-bp fragment (246 bp of exon1 plus 6 bp of exon2) was cloned into pAcGFP-N1 (Clontech) to generate a wild-type *mll* (exon1)-GFP fusion protein expression vector (WT2). A mutated *mll*(exon1)-GFP fusion protein expression vector (MT2) was generated by PCR using a forward primer with 5 mismatched nucleotides: 5′-atcca**cc**g**tt**gcgca**aga**aggcagagtgt-3′ (five mismatched nucleotides are underlined).

Semi-quantitative RT-PCR—The primers used for amplifying zebrafish *scl, lmo2, gata1, pu.1, runx1,* c-*myb, flk1*, *gadd45αa* and *β-actin* are listed in supplemental Table 1. The procedure for semi-quantitative RT-PCR was described previously (40).

Rescue Experiments—The full-length wild-type *hoxb4a*, *hoxb7a, hoxb6b, hoxa9a,* and *hoxd3a* were PCR-amplified from a zebrafish cDNA pool and then subcloned into the Psp64 poly(A) vector (Promega). Synthesized mRNA was injected into embryos at 100 pg/per embryo. The primers are listed in supplemental Table 1.

Luciferase Reporter Assay and mRNA Injection—The 1360-bp promoter of zebrafish *gadd45αa* (previously named *gadd45αl*) was PCR-amplified from wild-type zebrafish genomic DNA using the primers listed in supplemental Table 1 and then subcloned into the pGL3-Basic vector (Promega).

For *MLL* overexpression, 20–30 one-cell stage embryos were injected either with the PCNX-human MLL expression vector (5 pg/per embryo) (provided by Stanley Korsmeyer) combined with the pGL3-*gadd45αa* promoter vector (0.1 pg/per embryo) and *CMV-Renilla* (0.1 pg/per embryo, as an internal control) or with empty vector (5 pg/per embryo) combined with the pGL3-*gadd45αa*-promoter (0.1 pg/per embryo) and *CMV-Renilla* (0.1 pg/per embryo). For *mll* knockdown, 20–30 one-cell stage embryos were injected either with *mll*-MO1 (8 ng/per embryo) combined with pGL3-*gadd45αa*-promoter vector (0.1 pg/per embryo) and *CMV-Renilla* (0.1 pg/per embryo) or with control MO (8 ng/per embryo) combined with pGL3-*gadd45αa*-promoter (0.1 pg/per embryo) and *CMV-Renilla* (0.1 pg/per embryo). After 12 h, embryos were homogenized, and luciferase activity measurements were taken by a Dual-Luciferase reporter assay system (Promega).

For *gadd45αa* mRNA injection experiments, the full-length cDNA of zebrafish *gadd45αa* was amplified and then subcloned into the Psp64 poly(A) vector (Promega). Synthesized mRNA was injected into embryos at 400 pg/per embryo. The primers are listed in supplemental Table 2.

RESULTS

Amino Acid Sequence of Zebrafish mll Is Evolutionarily Conserved with Mammalian MLL—Using the GenBank™ data base, we identified the zebrafish ortholog of the *MLL* gene (accession number NM_001110279). *Mll* contains 12,703-bp nucleotides and encodes a protein 4218 amino acids in length, which is longer than that of the human MLL protein (3969 amino acids).

As showed in supplemental Fig. 1, zebrafish *mll* encodes most all of the functional domains identified in the mammalian *MLL* gene, including the AT hook motifs, a C*XXC* zinc-finger domain, a central zinc finger (PHD) region, and a C-terminal SET domain. The functional domains of the human and zebrafish *mll* gene share a high degree of identity as follows:

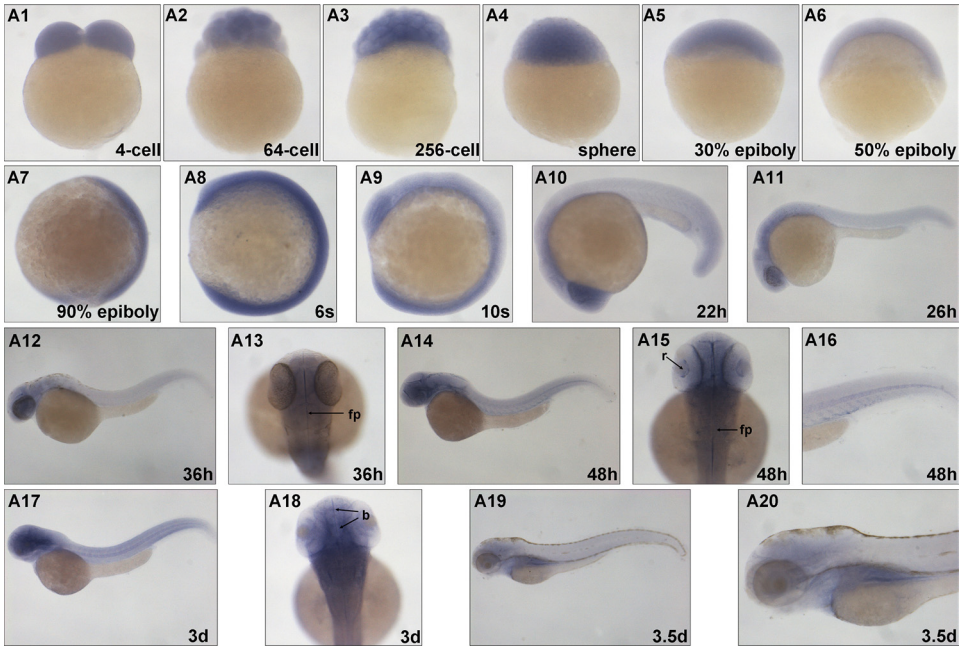

FIGURE 1. **Developmental expression of zebrafish *mll*.** Whole mount *in situ* hybridization analysis of zebrafish *mll* expression (*blue*) at the 4-cell (lateral view), 64-cell (lateral view), 256-cell (lateral view), sphere (lateral view), 30% epiboly (lateral view), 50% epiboly (lateral view), 90% epiboly (lateral view), 6-somite (lateral view), 10-somite (lateral view), 22-hpf (lateral view), 26-hpf (lateral view), 36-hpf (lateral view), 36-hpf (dorsal view), 48-hpf (lateral view), 48-hpf (dorsal view), 48-hpf (tail, dorsal view), 3-dpf (lateral view), 3-dpf (dorsal view), and 3.5-dpf (lateral view) stages. *s*, somite; *h*, hours post-fertilization; *d*, days post-fertilization; *fp*, floor plate; *r*, retina.

63.64% in AT1 and AT2, 77.78% in AT3, 93.88% in C*XXC*, 78.85% in PHD1, 83.64% in PHD2, 69.35% in PHD3, 71.74% in Bromo, and 85.21% in the SET domain. Compared with the whole protein sequence that shares 51.8% identity, the functional domains of the human and zebrafish proteins show a much higher level of conservation. Zebrafish *Mll* also contains the two identical proteolytic cleavage sites (Taspase1) found in human and mouse proteins, suggesting that zebrafish Mll also undergoes proteolytic processing into the MLL^N and MLL^C fragments *in vivo*.

Zebrafish mll Is Expressed Ubiquitously during Early Embryogenesis—We evaluated the expression patterns of *mll* during embryo development using whole mount *in situ* hybridization (Fig. 1). At early developmental stages, *mll* expression was ubiquitous in all cells, suggesting a maternal expression (Fig. 1, *A1–A9*). By 22 h post-fertilization (hpf), the *mll* expression pattern appeared as a gradient, from the anterior head region to the posterior tail (Fig. 1, *A10–A13*). The anterior head region expressed the highest level of *mll* with a slight decrease in the anterior trunk region attached to the yolk sac. Other regions of the body expressed lower homogenous *mll* levels (Fig. 1, *A10–A13*). By 48 hpf, the anterior head region continued to express the highest levels with a relatively high level of *mll* expression also found along the blood vessels (Fig. 1, *A14–A16*). This expression pattern could last up to 3 days post-fertilization (dpf). However, by 3.5 dpf, the highest expression of *mll* occurred in the kidney region. Although the anterior head region still expressed *mll*, its expression was not detected in other regions of body (Fig. 1, *A19–A20*).

Zebrafish mll Is Essential for Early Embryo Development and Hematopoiesis—To investigate the roles of *mll* during zebrafish embryogenesis, we depleted its expression in zebrafish embryos using morpholino (MO)-mediated gene-knockdown. We totally designed three morpholinos based on the cDNA sequence and linkage sequence between exon1 and intron1 of zebrafish *mll* gene as follows: one blocked *mll* translation by targeting the ATG site (*mll*-MO1); another one blocked *mll* splicing by targeting the linkage sequence between exon1 and intron 1 (*mll*-MO2), and the third one blocked *mll* translation by targeting 5′-UTR region (*mll*-MO3) (Fig. 2*A*).

For validation of *mll*-MO1, we used RT-PCR to clone a cDNA fragment that partially encompassed the 5′-UTR (*mll*-MO1-targeted region) along with exon1 into pAcGFP-N1 (Clontech) to generate a wild-type *mll* (exon1)-GFP fusion protein expression vector (named as WT1). We also generated a mutated *mll* (exon1)-GFP fusion protein expression vector (named as MT1, with seven mismatched nucleotides in the *mll*-MO1-targeting region). We co-injected embryos with *mll*-MO1 (8 ng/per embryo) and either WT1 or MT1 vector. *Mll*-MO1 efficiently blocked expression from the WT1 but not MT1 vector (Fig. 2, *panels B*2 and *B4*). However, the control MO (control), a standard morpholino described previously (41), could not block expression from either vector (Fig. 2, *panels B1* and *B3*). These observations indicate that *mll*-MO1 could knock down zebrafish *mll* expression during embryogenesis efficiently and specifically.

For validation *mll*-MO2, we designed three primers (P1, P2, and P3) for RT-PCR analysis (Fig. 2, *panels C1* and *C2*). After injecting embryos with control MO (8 ng/per embryo) or *mll*-MO2 (8 ng/per embryo), we performed RT-PCR. The results showed that *mll*-MO2 injection could generate a DNA fragment with the size as predicted (976 bp, named F2) (Fig. 2, *panel C3*), which was further verified by sequencing (data not shown).

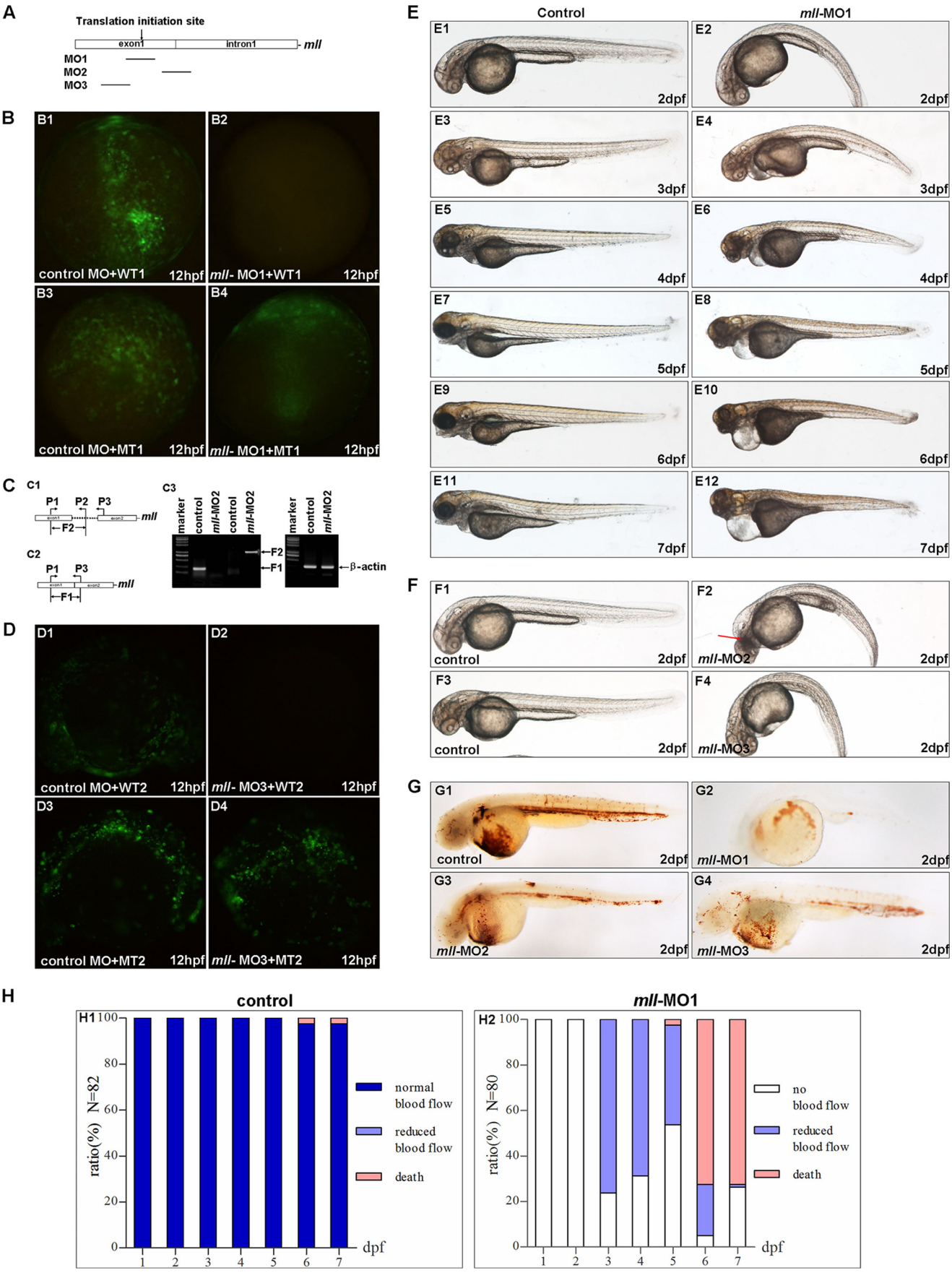
A
Translation initiation site
exon1
intron1
mll
MO1
MO2
MO3
B
B1
control MO+WT1 12hpf
B2
mll- MO1+WT1 12hpf
B3
control MO+MT1 12hpf
B4
mll- MO1+MT1 12hpf
C
C1
P1 P2 P3
mll
F2
C2
P1 P3
mll
F1
C3
marker
control
mll-MO2
control
mll-MO2
F2
F1
marker
control
mll-MO2
β-actin
D
D1
control MO+WT2 12hpf
D2
mll- MO3+WT2 12hpf
D3
control MO+MT2 12hpf
D4
mll- MO3+MT2 12hpf
E
Control
mll-MO1
E1 2dpf
E2 2dpf
E3 3dpf
E4 3dpf
E5 4dpf
E6 4dpf
E7 5dpf
E8 5dpf
E9 6dpf
E10 6dpf
E11 7dpf
E12 7dpf
F
F1 control 2dpf
F2 mll-MO2 2dpf
F3 control 2dpf
F4 mll-MO3 2dpf
G
G1 control 2dpf
G2 mll-MO1 2dpf
G3 mll-MO2 2dpf
G4 mll-MO3 2dpf
H
control
H1
ratio(%) N=82
100
80
60
40
20
0
1 2 3 4 5 6 7
dpf
normal blood flow
reduced blood flow
death
mll-MO1
H2
ratio(%) N=80
100
80
60
40
20
0
1 2 3 4 5 6 7
dpf
no blood flow
reduced blood flow
death

These results indicated that *mll*-MO2 could block *mll* splicing efficiently and specifically.

For validation *mll*-MO3, we used the same approach as that for validating *mll*-MO1. As showed in Fig. 3*D*, *mll*-MO3 could also knock down *mll* expression efficiently and specifically.

Subsequently, we investigated the effect of *mll* knockdown mediated by morpholino injections during zebrafish embryogenesis. In 10 independent experiments, injection of *mll*-MO1 (8 ng/per embryo) into zebrafish embryos produced obvious defects in embryogenesis and hematopoiesis (Fig. 1*E*). Of note, the embryos injected with *mll*-MO1 showed a similar morphology to that of the embryos injected with the control MO (8 ng/per embryo) up until 26 hpf, the time at which embryonic blood flow normally begins (data not shown). From 2 dpf, we observed significant defects in the *mll*-MO1 morphants, including curved body axis, heart edema, reduced blood cells, and a lack of blood flow (Fig. 2, *panels E1–E10,* and data not shown). At 7 dpf, control embryos continued to show normal development (Fig. 2, *panel E11*), whereas *mll*-MO1 morphants had shorter bodies, smaller eyes, serious heart edema, and still no blood flow (Fig. 2, *panel E12,* and data not shown). All *mll*-MO1 morphants died between 6 and 10 dpf (Fig. 2, *panel H2*). As predicted, injection of *mll*-MO2 or *mll*-MO3 generated similar phenotypes as that of *mll*-MO1 (Fig. 2*F*) except that *mll*-MO2 injection caused more degeneration in the head region (Fig. 2, *panel F2,* indicated by *red arrow*). These observations further suggest that all three morpholinos could knock down *mll* expression efficiently and specifically, and *mll*-MO2 might have some additional nonspecific effects.

Given that previous studies have shown an important role for *MLL* in mammalian hematopoiesis (6, 7) and the obvious defects in blood cell number and blood flow we observed in *mll* morphants, we next focused on investigating the influence of *mll* on zebrafish hematopoiesis. We first traced blood flow in morphants from 2 to 7 dpf under a dissection microscope. Interestingly, blood flow partially recovered with reduced circulatory blood cells in 78% of morphants injected with 8 ng/per embryo *mll*-MO1 ($n = 80$) at 3 dpf (Fig. 2, *panel H2,* and data not shown), but then gradually decreased after 4 dpf (Fig. 2, *panel H2*). In 7-dpf morphants, blood flow completely ceased (data not shown). When alive, the *mll*-MO1 morphants had either no blood cells or only one clump of blood cells located back and in front of beating hearts, whereas control embryos developed normally both in terms of morphology and blood flow. No recovery of blood flow occurred in embryos injected with a higher concentration *mll*-MO1 (12 ng/per embryo) (data not shown). Moreover, an *mll*-MO1 concentration of 16 ng/per embryo resulted in embryonic death at 2 dpf (data not shown). These observations not only suggest that *mll*-MO1 affected zebrafish embryogenesis and hematopoiesis in a dose-dependent manner but also imply that the low concentration of *mll*-MO1 could completely block definitive hematopoiesis, but only partially block primitive hematopoiesis.

To further determine the role of *mll* in zebrafish erythropoiesis, *o*-dianisidine staining for hemoglobin was performed to check whether red cell maturation was affected by *mll* knockdown. The results indicated that the mature red blood cells were dramatically reduced in *mll*-depleted embryos mediated by all three morpholino injections compared with control embryos at 2 dpf (Fig. 2*G*).

In all *mll*-MO1, *mll*-MO2, and *mll*-MO3 morphants, particularly in *mll*-MO2 morphants, we observed obscured areas in

FIGURE 2. **Knockdown of *mll* by morpholinos (*mll*-MO1, *mll*-MO2, and *mll*-MO3) caused defects in erythropoiesis, blood circulation, and morphogenesis.** *A,* schematic diagram depicts the targets of three morpholinos in zebrafish *mll* genome. *B,* validation of *mll*-MO1. *Panel B1,* embryos were injected with control MO (8 ng/per embryo) and a wild-type *mll* (exon1)-GFP fusion protein expression vector (WT1) (5 pg/per embryo) and then examined by fluorescence microscopy. *Panel B2,* embryos were injected with *mll*-MO1 (8 ng/per embryo) and a wild-type *mll* (exon1)-GFP fusion protein expression vector (WT1) (5 pg/per embryo) and then examined by fluorescence microscopy. *Panel B3,* embryos were injected with control-MO (8 ng/per embryo) and a mismatch-mutated *mll*-GFP fusion protein expression vector (MT1) (5 pg/per embryo) and then examined by fluorescence microscopy. *Panel B4,* embryos were injected with *mll*-MO1 (8 ng/per embryo) and a mismatch mutated *mll* (exon1)-GFP fusion protein expression vector (MT1) (5 pg/per embryo) and then examined by fluorescence microscopy. *C,* validation of *mll*-MO2. *Panel C1*, schematic diagram depicts the genomic fragment of *mll* exon1, intron1, and exon2. The positions of PCR primers used to detect fragment 2 (*F2*) are indicated by *arrows*. *Panel C2*, schematic diagram depicts the cDNA fragment of *mll* exon1 and exon2. The positions of PCR primers to detect fragment 1 (*F1*) are indicated by *arrows*. *Panel C3,* gels show that *mll*-MO2 (8 ng/per embryo) blocked splicing of exon1 and exon2 of *mll* efficiently. The fragment 1 resulting from normal splicing was not detected in embryos injected with *mll*-MO2 (8 ng/per embryo) as indicted in *3rd line* (from *left* to *right, left panel*), but it was detected in embryos without injection (control) as indicated in *2nd line* (from *left* to *right, left panel*). Fragment 2 resulting from blocking splicing was detected in embryos injected with *mll*-MO2 (8 ng/per embryo) as indicated in *5th line* (from *left* to *right*, *left panel*), but it was not detected in embryos without injection (control) as indicated in *4th line* (from *left* to *right, left panel*). The cDNA fragment of β-actin can be detected in both control embryos and *mll*-MO2 morphants as indicted in *2nd* and *3rd lines* (from *left* to *right, right panel*). *D,* validation of *mll*-MO3. *Panel D1*, embryos were injected with control-MO (8 ng/per embryo) and a wild-type *mll*(exon1)-GFP fusion protein expression vector (*WT2*) (5 pg/per embryo) and then examined by fluorescence microscopy. *Panel D2,* embryos were injected with *mll*-MO3 (8 ng/per embryo) and a wild-type *mll* (exon1)-GFP fusion protein expression vector (WT2) (5 pg/per embryo) and then examined by fluorescence microscopy. *Panes D3,* embryos were injected with control-MO (8 ng/per embryo) and a mismatch-mutated *mll*-GFP fusion protein expression vector (MT2) (5 pg/per embryo) and then examined by fluorescence microscopy. *D4,* embryos were injected with *mll*-MO3 (8 ng/per embryo) and a mismatch mutated *mll* (exon1)-GFP fusion protein expression vector (MT2) (5 pg/per embryo) and then examined by fluorescence microscopy. *E,* morphological defects in *mll*-MO1 morphants. *Panel E1,* 2-dpf embryos without morpholino injection (control) developed normally. *Panel E2, mll*-MO1 morphants (2-dpf stage) showed a curved body and heart edema. *Panel E3,* 3-dpf embryos without morpholino injection (control) developed normally. *Panel E4, mll*-MO1 morphants (3-dpf stage) showed heart edema and a shortened body. *Panel E5,* 4-dpf embryos without morpholino injection (control) developed normally. *Panel E6, mll*-MO1 morphants (4-dpf stage) showed severe heart edema, smaller eyes, and a shortened body. *Panels E7, E9,* and *E11,* 5–7-dpf embryos without morpholino injection (control) developed normally. *Panels E8, E10* and *E12, mll*-MO1 morphants (5–7-dpf stage) showed severe heart edema, smaller eyes, a shortened body, and an abnormal head. *F,* morphological defects in *mll*-MO2 and *mll*-MO3 morphants. *Panel F1,* 2-dpf embryos without morpholino injection (control) developed normally. *Panel F2, mll*-MO2 morphants (2-dpf stage) showed a curved body and head degenerated. *Panel F3,* 2-dpf embryos without morpholino injection (control) developed normally. *Panel F4, mll*-MO3 morphants (2-dpf stage) showed a curved body and heart edema. *G,* defects of erythropoiesis in *mll* morphants. *Panel G1,* erythropoiesis in embryos (2-dpf stage) without morpholino injection was normal as revealed by *o*-dianisidine staining for hemoglobin. *Panel G2,* erythropoiesis in embryos (2-dpf stages) injected with *mll*-MO1 (8 ng/per embryo) was blocked as revealed by *o*-dianisidine staining for hemoglobin. *Panel G3,* erythropoiesis in embryos (2-dpf stages) injected with *mll*-MO2 (8 ng/per embryo) was blocked as revealed by *o*-dianisidine staining for hemoglobin. *Panel G4,* the erythropoiesis in embryos (2-dpf stages) injected with *mll*-MO3 (8 ng/per embryo) was blocked as revealed by *o*-dianisidine staining for hemoglobin. *H,* quantitative assays for blood circulation in embryos. *Panel H1,* different stage embryos without morpholino injection showed normal blood flow. *Panel H2,* different stage *mll*-MO1 morphants showed no blood flow or reduced blood flow.

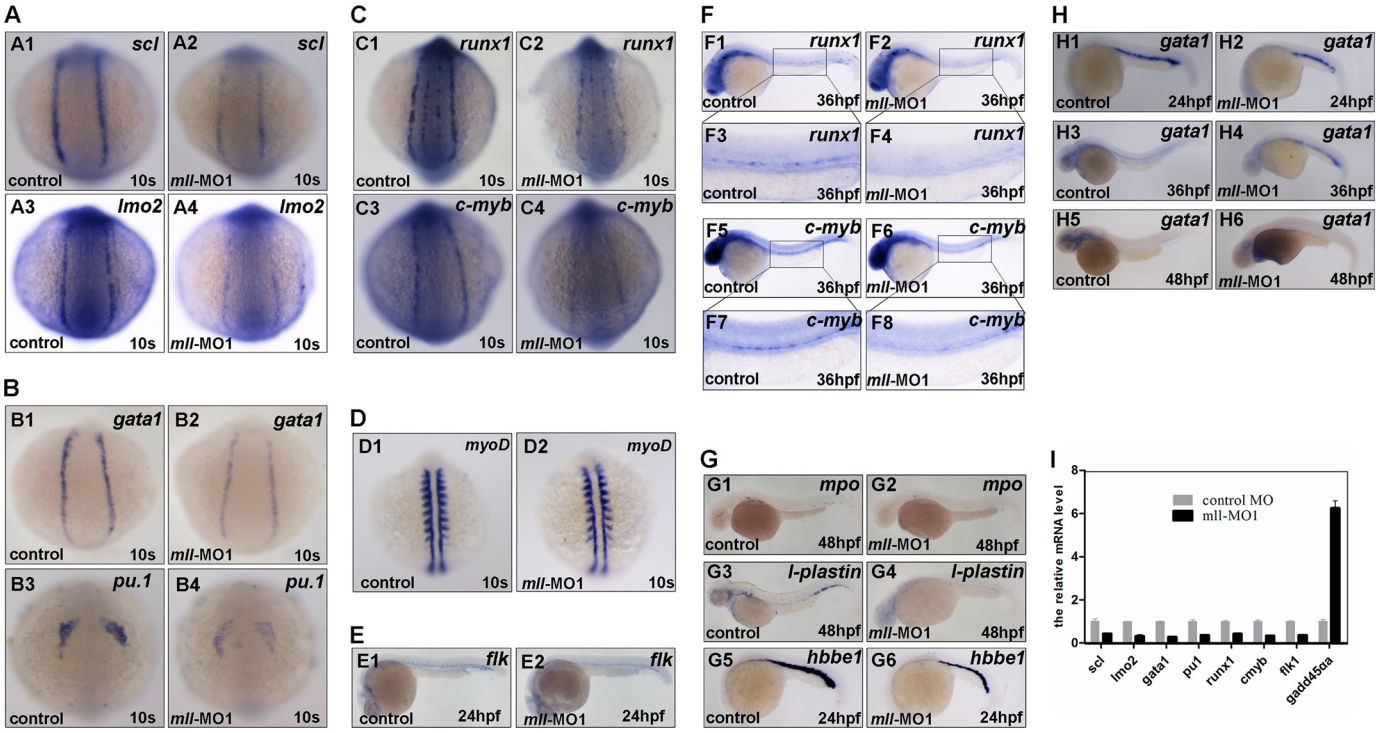

FIGURE 3. ***mll* is required for embryonic and adult hematopoietic marker gene expression.** Whole mount *in situ* hybridization assays for hematopoiesis markers in control embryos or *mll*-MO1-injected embryos. *A,* expression patterns of *scl* and *lmo2 in* control embryos or *mll*-MO1 morphants at the 10-somite stage. *Panels A1* and *A2, scl*; *A3* and *A4, lmo2*. *B,* expression patterns of *gata1* and *pu.1* in control embryos or *mll*-MO1 morphants at 10-somite stage; *Panels B1* and *B2, gata1*; *B3* and *B4, pu.1*. *C,* expression patterns of *runx1* and c-*myb* in control embryos or *mll*-MO1 morphants at 10-somite stage, *Panels C1* and *C2, runx1*; *C3* and *C4,* c-*myb*. *D,* expression patterns of *myoD* in control embryos (*panel D1*) or *mll*-MO1 morphants (*panel D2*) at 10-somite stage. *E,* expression patterns of *flk1* in control embryos or *mll*-MO1 morphants at 24-hpf stage. *F,* expression patterns of *runx1* and c-*myb* in control embryos or *mll*-MO1 morphants at 36-hpf stage. *Panels F1–F4, runx1*; and *F5–F8,* c-*myb*. *G,* expression patterns of *mpo, l-plastin,* and *hbbe1* in control embryos or *mll* morphants at 48-hpf stage. *Panels G1* and *G2, mpo*; *G3* and *G4, l-plastin*; and *G5* and *G6, hbbe1*. *H, Gata1* expression in embryos without *mll*-MO1 injection at 24-, 36-, and 48-hpf stages. *Panels H1, H3* and *H5, gata1* expression in embryos without *mll*-MO1 injection; *panels H2, H4,* and *H6, gata1* expression in *mll*-MO1 morphants. *s*, somites; *hpf,* hours post-fertilization. *I,* semi-quantitative RT-PCR analysis for the expression regulation of *scl, lmo2, gata1, pu.1, runx1,* c-*myb, flk1,* and *gadd45αa* by *mll* knockdown using *mll*-MO1 at 10-somite stage.

the head and trunk regions, indicating tissue degeneration (Fig. 2, *E* and *F,* and data not shown). Further apoptosis staining showed that *mll*-MO1 and *mll*-MO2 injection could indeed induce apoptosis in embryos compared with control MO injection, particularly for *mll*-MO2 injection (supplemental Fig. 2*A*). This apoptosis induction could be the result from off-target effect of morpholinos (42). To test this possibility, we co-injected embryos with a morpholino directed against *p53* (*p53*-MO) combined with *mll*-MO1, *mll*-MO2, or *mll*-MO3, respectively, and then compared these embryos with those injected with *mll*-MO1, *mll*-MO2, or *mll*-MO3 alone. The embryos with the *p53*-MO/*mll*-MO combined injection became much more transparent and had less apoptotic cells than those injected with *mll*-MO1, *mll*-MO2, or *mll*-MO3 alone (data not shown); however, the defects in hematopoiesis remained unchanged (data not shown).

To further figure out whether the defects in hematopoiesis exhibited in *mll* morphants resulted from the influence of *mll* on cell proliferation, we performed phosphorate-histone H3 staining (43). As shown in supplemental Fig. 2*B*, the cell proliferation was not altered obviously in *mll* morphants as revealed by phospho-H3 immunofluorescent staining. Together, these observations support the specificity of *mll* morpholinos for mediating *mll* knockdown and the important roles of *mll* on hematopoiesis.

Mll Is Required for Maintaining Hematopoietic Progenitors and for Proper Erythroid and Myeloid Formation—To better understand how *mll* knockdown led to blood cell reduction and blood flow loss, we looked at expression of both hematopoietic cell markers and vascular markers. As shown in Fig. 3*A* and supplemental Fig. 3*B*, *mll*-MO1 morphants at the 5- and 10-somite stage (10 s) dramatically down-regulated expression of the early hemangioblast markers, s*cl* and *lmo2* (Fig. 3, *panels A1–A4, and* supplemental Fig. 3, *panels B1–B4*), whereas the pronephric duct marker *pax2a* and precardiac marker *nkx2.5* were not altered in the lateral plate mesoderm (supplemental Fig. 3*A*). *gata1* and *pu1*, markers for erythroid and myeloid progenitors, respectively, were also reduced in morphants at 10-somite stage (Fig. 3, *panels B1–B4*). In addition, morphants had a decrease in expression of the hematopoietic progenitor marker *runx1* as well as c-*myb* at 10-somite stage (Fig. 3, *panels C1–C4*). These results suggest that *mll* depletion might specifically block the hematopoietic program but neither the pronephric cell lineage nor precardiac cell lineage.

To ensure that the alteration of hematopoietic markers in *mll*-MO1 morphants was not the result of the developmental delay usually observed in some morpholino injections, we used the myogenic marker *myoD* to monitor developmental stages. The results showed that mll-MO1 injection did not cause developmental delay (Fig. 3*D*).

Loss of blood flow might result from a defect in vasculature development, a blood deficiency, or both. To explore the real cause, we checked expression of the vascular endothelial cell marker *flk1* and aorta marker *ephB2a*. As shown in Fig. 3*E* and supplemental Fig. 4*A*, both *flk1* and *ephB2a* were indeed reduced in *mll*-depleted embryos. However, they were still expressed in *mll*-MO1 morphants at the 24- or 36-hpf stage, respectively. To further understand whether vascular development was affected by *mll* knockdown, we used tracing experiments by taking advantage of *flk*-GFP transgenic fish (GFP expression driven by *flk* promoter) and found that the formation of vessels was not defected in morphants by 24 hpf (supplemental Fig. 4, *panels B1–B4*). Of note, by 36 hpf, the lateral vessels gradually began to recover, from the anterior to the posterior (supplemental Fig. 4, *panels B5* and *B6*), and then by 48 hpf they were almost fully recovered (supplemental Fig. 4, *panels B7* and *B8*). These observations indicate that the loss of blood flow in morphants resulted from hematopoietic deficiency rather than a defect of vasculature development.

To further confirm that definitive hematopoiesis was also affected by *mll* knockdown, we checked expression of *runx1* and c-*myb* at the 36-hpf stage. As shown in Fig. 3*F*, both *runx1* and c-*myb* were reduced in *mll*-MO1 morphants. These observations suggest that *mll* plays an important role in definitive hematopoiesis as well as that in primitive hematopoiesis.

As expected, mature hematopoietic cell markers, such as *mpo* (granulocytes), *l-plastin* (macrophage), and *hbbe1* (red blood cells), were all significantly reduced, but not absent, in morphants at 24 or 48 hpf (Fig. 3*G*). Interestingly, at 24 hpf, the *mll*-MO1 morphants had a reduced level of erythroid progenitors marked by *gata1* (Fig. 3, *panels H1* and *H2*); however, at 36 hpf, the *gata1*-positive cells were still gathered at the intermediate cell mass of Oellacher region in morphants, whereas in control embryos the *gata-1*-positive cells disappeared (Fig. 3, *panels H3* and *H4*). Even in 48-hpf *mll*-MO1 morphants, the *gata1*-positive cells still could be found around the heart area (Fig. 3, *panels H5* and *H6*). Given that the red blood cells had already matured and entered into the blood circulation at 36 hpf, we hypothesize that *mll* depletion might also block erythroid progenitor differentiation in addition to preventing erythroid progenitor formation.

To further confirm the similar effect of *mll*-MO2, we performed all markers staining as well as that for *mll*-MO1. The result showed that *mll*-MO2 could cause alteration of gene expression similar to that of *mll*-MO1 (supplemental Fig. 5 and data not shown). As expected, *mll*-MO3 caused the alteration of all marker expression that was similar to that of *mll*-MO1 (data not shown). These observations further confirm the specificity and efficiency of these three *mll* morpholino-mediated *mll* knockdowns.

Taken together, these observations suggest that *mll* is required for maintaining hematopoietic progenitors and for proper erythroid and myeloid formation. Gene expression changes after *mll* knockdown mediated by *mll*-MO1 injection were confirmed by semi-quantitative RT-PCR (Fig. 3*I*).

Mll N-terminal Mini-peptide Disrupts Normal Function of mll—Interestingly, in performing validation experiments for *mll*-MO1, we noticed that whenever we injected *mll* (exon1)-GFP vector (named WT1 that contained the 17-bp UTR region plus 246-bp exon1 and 6-bp exon2 of zebrafish *mll*) into embryos, the embryos exhibited phenotypes quite similar to that of *mll* morphants if not identical, including shorter body, smaller eyes, heart edema, reduced blood cells, and no blood flow (data not shown). After examining the sequence of WT1, we realized that it encoded an 84-amino acid peptide fused with GFP, which contains 82 amino acids of *mll* exon1 and -2 amino acids of *mll* exon2. This phenomenon led us to hypothesize that the 84-amino acid N terminus of zebrafish *mll* might function as a dominant negative form of *mll* in affecting hematopoiesis and embryogenesis. The sequence alignment analysis for the 82-amino acid N terminus of *mll* among human, mouse, and zebrafish indicated that the N terminus of *mll* was evolutionarily conserved, particularly for the first 14 amino acids (100% identical), which has been identified for Menin binding previously (Fig. 4*A*) (44). To further test this hypothesis, we synthesized an mRNA encoding 84 amino acids of the *mll* N terminus and did mRNA injection assays. After this mRNA was injected into embryos at the one cell stage (400 pg/per embryo), the embryos displayed a smaller body size, shortened body axis, degenerated head region, cardiac edema, as well as a lack of blood flow (Fig. 4*B* and data not shown). These phenotypes were very similar, if not identical, to that of the *mll* morphants. In addition, we examined the expression of hematopoietic markers *scl, gata1,* and *pu.1* (Fig. 4*C*), precardiac marker *nkx2.5* (Fig. 4, *panels D1* and *D2*), pronephric duct marker *pax2a* (Fig. 4, *panels D3* and *D4*), and myogenic marker *myoD* (Fig. 4, *panels D5* and *D6*) after an 84-amino acid mRNA injection. The alteration of the above markers by an 84-amino acid mRNA injection exhibited a similar changing tendency to that of *mll* morpholino injections (Fig. 4, *C* and *D*). These data implicate that the N terminus of *mll* may function as a dominant negative form of *mll*, which disrupts normal function of *mll* during embryogenesis and hematopoiesis.

Mll Depletion Altered Hox Gene Expression and hoxa9a and hoxd3a Partially Rescued the Formation of Early Hematopoietic Progenitors—Studies have demonstrated a well defined role for *Mll* in regulating the expression of a cluster of *Hox* genes, many of which participate in mammalian hematopoiesis (27, 28, 30, 45–48). Therefore, we next asked whether *mll* knockdown affected expression of the genes *hoxa9a*, *hoxc8*, *hoxb7a*, *hoxb6b*, *hoxb4*, and *hoxd3a* or expression of their upstream gene *cdx4*. As shown in Fig. 5, *mll*-MO1 morphants exhibited a dramatic down-regulation of *hoxa9a*, *hoxb4a*, *hoxb6b,* and *hoxd3a*, but there was no obvious change in the expression of *hoxb5a, hoxb7a, hoxc8,* and *cdx4* (supplemental Fig. 6). Similar results were obtained by *mll*-MO2 injection (Fig. 5*B* and data not shown).

We then performed rescue experiments to determine whether the *mll*-MO1-mediated effect on hematopoiesis was the result of *Hox* gene down-regulation. For these experiments, we synthesized *hoxa9a, hoxb4a, hoxb7a, hoxb6b,* and *hoxd3a* mRNA and then co-injected embryos with each of the *Hox* mRNAs (100 pg/per embryo) and *mll*-MO1 (8 ng/per embryo). Whole mount *in situ* hybridization showed that only *hoxa9a* and *hoxd3a* mRNA could partially rescue expression of the early hematopoietic progenitor markers *scl*, *gata1,* and *pu.1*

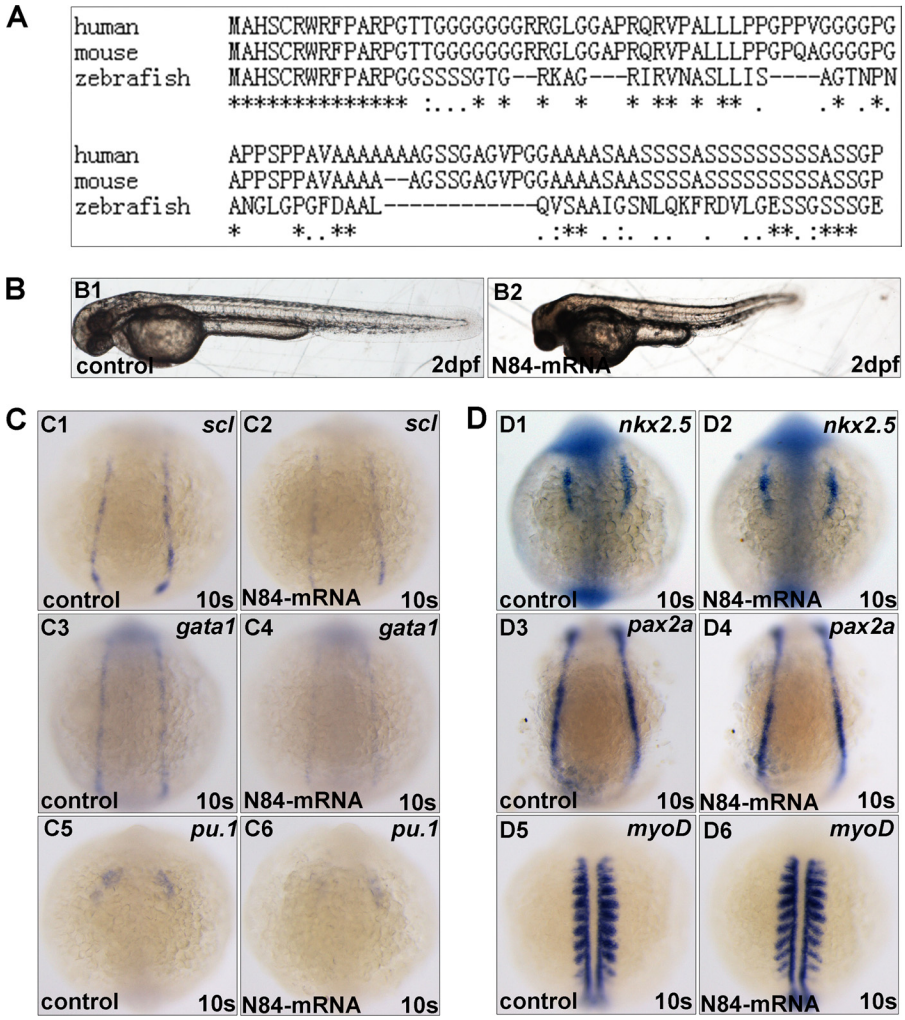

FIGURE 4. **Overexpression of the zebrafish *mll* N-terminal 84-amino acid peptide (exon1 plus 2 amino acids of exon2) in embryos caused defects in hematopoiesis similar to that observed in *mll* morphants.** *A,* alignment of 82 amino acids (exon1) in N terminus of zebrafish *mll* with its human and mouse orthologs. *B,* morphology of embryos without injection (control) or injected with mRNA encoding 84 amino acids of *mll* exon1. *C,* expression patterns of *scl, gata1,* and *pu.1* in embryos without injection (*control*) or injected with mRNA of 84-amino acid peptide at 10-somite stage. *Panels C1* and *C2, scl*; *panels C3* and *C4, gata1*; *panels C5* and *C6, pu.1*. *D,* expression patterns of *nkx2.5, pax2a,* and *myoD*. *Panels D1* and *D2, nkx2.5*; and *panels D3* and *D4, pax2a*; and *panels D5* and *D6, myoD*. *s,* somite.

(Fig. 6, *A3, A7,* and *A11* and *A4, A8,* and *A12*) (for *hoxoa9a*, n = 32/78; for and rabbit anti, n = 36/87) but not *hoxb7a*, *hoxb6b*, and *hoxb4a*, (supplemental Fig. 6*B*), which were further confirmed by semi-quantitative RT-PCR assays (data not shown). However, none of the *Hox* mRNAs rescued blood flow (data not shown). Although the ability of *mll* to target *hoxd3a* and *hoxa9a* expression may contribute to hematopoietic regulation, these results suggest the involvement of other *mll* targets as well.

To further determine whether *hoxa9a* or *hoxd3a* knockdown could recapitulate the phenotypes of *mll* morphants, we injected *hoxa9a*-MO (8 ng/per embryo) (CGACAATTTGGTCAGCTTACCTGGA; splicing-blocking) or *hoxd3a*-MO (8 ng/per embryo) (CATAATAAGTGGCTTTCTGCATTGC; translation-blocking) into one-cell stage embryos, respectively. The results showed that either *hoxa9a*-knockdown or *hoxd3a*-knockdown reduced red blood cell number partially (*hoxa9a* morphants, 35%, n = 108; *hoxd3a* morphants, 33.7%, n = 83). No other obvious phenotypes were observed (data not shown). These results further suggest that *hoxa9a* and *hoxd3a* could only partially account for the role of *mll* in embryogenesis, even in hematopoiesis.

Gadd45αa Is a Potential mll Target Involved in Zebrafish Hematopoiesis—To better understand the underlying mechanism of how *mll* regulates hematopoiesis, we performed expression profiling in *mll* morphants (10-somite stage) using a zebrafish oligonucleotide microarray representing about 44,000 genes (Agilent). To reduce the noise in the microarray data, we performed four parallel experiments using *mll*-MO1 and *mll*-MO2. We considered genes whose average fold change in expression was bigger than or equal to 2 in both *mll*-MO1 and *mll*-MO2 morphants as *mll*-regulated targets. As shown in supplemental Table 2, after knockdown of full-length *mll* we identified 27 known genes that were up-regulated and 45 that were down-regulated. Not surprisingly, most of down-regulated genes were related to hematopoiesis and neurogenesis, for example 4 *Hox* genes, *lmo2*, and *kdr1,* supporting the use of this microarray as an initial screen.

Based on this assay, we identified *gadd45αa* (previously named as *gadd45al*), as the gene with the highest fold increase

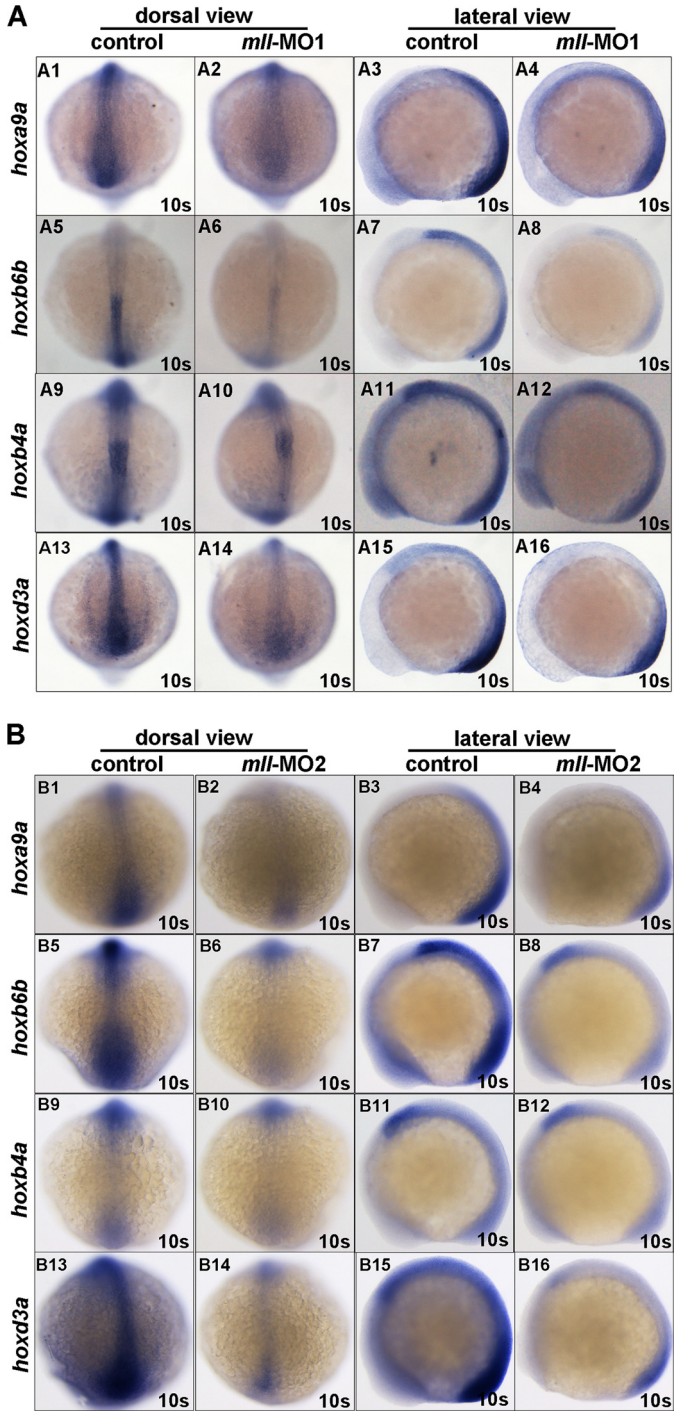

FIGURE 5. ***mll* is required for *Hox* gene expression.** Whole mount *in situ* hybridization assays for *Hox* gene expression in embryos without morpholino injection (*control*) or injected with *mll*-MO1 and *mll*-MO2 at 10-somite stage. *A, Hox* gene expression in embryos without morpholino injection (*control*) or injected with *mll*-MO1 at 10-somite stage. *Panels A1–A4, Hoxa9a* (dorsal view and lateral view); *panels A5–A8, Hoxb6b* (dorsal view and lateral view); *panels A9–A12, Hoxb4a* (dorsal view and lateral view); *panels A13–A16, Hoxd3a* (dorsal view and lateral view). *B, Hox* gene expression in embryos without morpholino injection (control) or injected with *mll*-MO2 at 10-somite stage. *Panels B1–B4, Hoxa9a* (dorsal view and lateral view); *panels B5–B8, Hoxb6b* (dorsal view and lateral view); *panels B9–B12, Hoxb4a* (dorsal view and lateral view); *panels B13–B16, Hoxd3a* (dorsal view and lateral view). *s*, somites.

in both *mll*-MO1 (6.98-fold) and *mll*-MO2 (224.44-fold) morphants. To confirm the up-regulation of *gadd45αa*, we performed whole mount *in situ* hybridization. In both *mll*-MO1 and *mll*-MO2 morphants, we observed an increase in *gadd45αa* expression as compared with the control (Fig. 7*A*, *panels A1–A3*). Semi-quantitative RT-PCR assays further confirmed that *gadd45αa* was up-regulated more than 6-fold after *mll* knockdown (Fig. 3*I*).

As shown above, the injection of *mll* morpholinos had some off-target effects for inducing cell apoptosis. In addition, it was reported previously that *gadd45α* is a p53-regulated stress protein (49). Thus, it is possible that *gadd45αa* up-regulation in *mll* morphants might be the result of p53 activation. To rule out this possibility, we co-injected *mll*-MO1 and *p53*-MO into zebrafish embryos and then looked at *gadd45αa* expression by whole mount *in situ* hybridization. The result showed that the up-regulation of *gadd45αa* in embryos with depleted *mll* and p53 was similar to that with only depleted *mll* (Fig. 7*A*, *panel A4*).

To further validate the suppressive role of *mll* on *gadd45αa*, we cloned a 1360-bp promoter of zebrafish *gadd45αa* into the pGL3-Basic vector to construct a luciferase reporter. As shown in Fig. 7*B*, *mll* overexpression significantly inhibited *gadd45αa* promoter activity ($p = 0.0067$), although *mll* knockdown significantly induced promoter activity ($p < 0.0001$). Furthermore, we checked the expression of *gadd45αb* (previously named as *gadd45α*), a homolog of zebrafish *gadd45αa*, in *mll* morphants. Unlike *gadd45αa*, *gadd45αb* expression was not altered after *mll* knockdown (Fig. 7*C*). Taken together, these observations suggest that *gadd45αa* might serve as a direct target of *mll*-mediated gene suppression in zebrafish.

We next asked if the targeting of *gadd45αa* by *mll* plays a role in hematopoiesis. We synthesized *gadd45αa* mRNA and then injected embryos (400 pg/per embryo). Embryos with overexpression of *gadd45αa* mRNA displayed defects in morphogenesis and hematopoiesis almost identical to the ones seen in the *mll* morphants, including small body size, curved body axis, heart edema, reduced blood cells, and lack of blood flow (Fig. 7*D* and data not shown). Whole mount *in situ* hybridization revealed a reduction of hematopoietic markers, including *scl, lmo2, gata1,* and *pu.1* in *gadd45αa*-overexpressing embryos (Fig. 7*F*) but not the pronephric marker *pax2a* (Fig. 7, *panels E3* and *E4*), similar to that observed in *mll* morphants. *MyoD* staining showed that *gadd45αa* mRNA injection also did not cause embryo development delay (Fig. 7, *panels E1* and *E2*). To obtain more evidence for supporting that *gadd45αa* is a target of *mll*, we designed and synthesized a morpholino for blocking *gadd45αa* translation by targeting its ATG code (*gadd45αa*-MO: CCGTTAAGTTCTTCAAAAGTCATGT) and then performed rescue experiments. As shown in Fig. 7*G*, *gadd45αa*-MO could indeed partially rescue hematopoietic marker *scl* and *gata1* expressions in *mll*-MO1 morphants (Fig. 7*G*; for *scl*, $n = 10/26$; for *gata1*, $n = 12/24$), which was further confirmed by semi-quantitative RT-PCR assays (data not shown). However, *gadd45αa*-MO injection could not rescue both blood flow and morphological deficiency exhibited in *mll* morphants, suggesting more downstream targets other than *Hox* genes and *gadd45αa* mediating the function of mll during embryogenesis.

Given that both *Hox* genes and *gadd45αa*-MO regulated by *mll*, we intended to figure out the relationship between

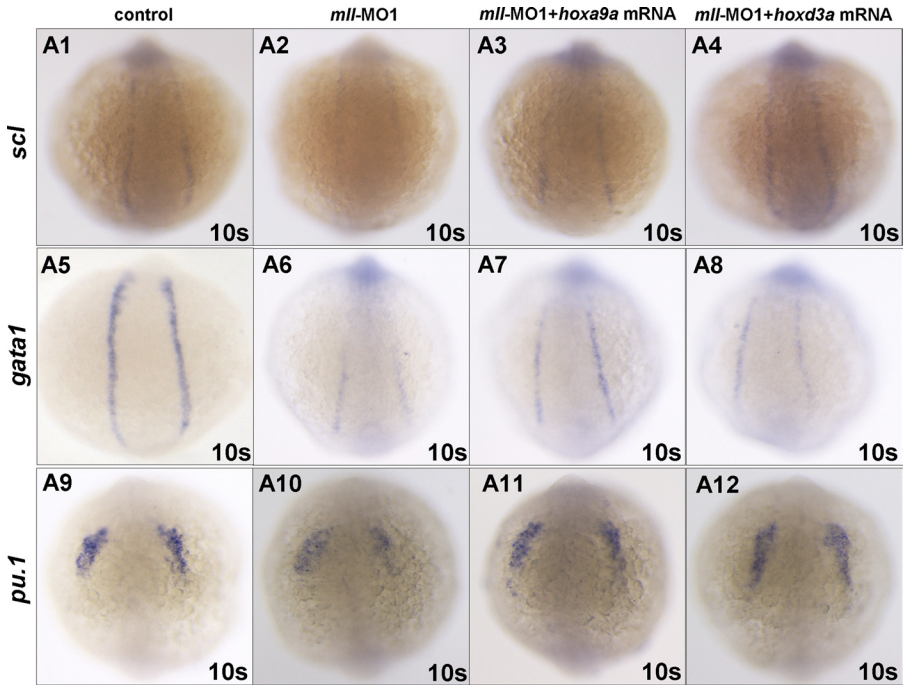

FIGURE 6. **Injection of either *Hoxa9a* mRNA or *Hoxd3a* mRNA could rescue *scl*, *gata1*, and *pu.1* gene expression in *mll*-MO1 morphants.** *A1*, *scl* expression in control embryos without *mll*-MO1 injection; *A2*, *scl* expression in *mll* morphants; *A3*, *scl* expression in embryos injected with *mll*-MO1 (8 ng/per embryo) combined with *Hoxa9a* mRNA (100 pg/per embryo); *A4*, *scl* expression in embryos injected with *mll*-MO1 (8 ng/per embryo) combined with *Hoxd3a* mRNA (100 pg/per embryo); *A5*, *gata1* expression in control embryos without *mll*-MO1 injection; *A6*, *gata1* expression in *mll* morphants; *A7*, *gata1* expression in embryos injected with *mll*-MO1 (8 ng/per embryo) combined with *Hoxa9a* mRNA(100 pg/per embryo); *A8*, *gata1* expression in embryos injected with *mll*-MO1 (8 ng/per embryo) combined with *Hoxd3a* mRNA (100pg/per embryo); *A9*, *pu.1* expression in control embryos without *mll*-MO1 injection; *A10*, *pu.1* expression in *mll* morphants; *A11*, *pu.1* expression in embryos injected with *mll*-MO1 (8 ng/per embryo) combined with *Hoxa9a* mRNA (100 pg/per embryo); *A12*, *pu.1* expression in embryos injected with *mll*-MO1 (8 ng/per embryo) combined with *Hoxd3a* mRNA (100 pg/per embryo).

gadd45αa and *Hox* genes. After embryos were injected with *hoxa9a*-MO or *hoxd3a*-MO, the expression of *gadd45αa* was not altered obviously (supplemental Fig. 7*A*). After embryos were injected with *gadd45αa* mRNA, neither *hoxa9a* nor *hoxd3a* was changed (supplemental Fig. 7*B*). Furthermore, *gadd45αa*-MO injection also did not alter *hoxa9a* and *hoxd3a* expression (data not shown). Taken together, these observations suggest that *gadd45αa* may serve as a *mll* target in regulating zebrafish hematopoiesis, and the regulation of *gadd45αa* by *mll* is parallel to that of *Hox* genes regulated by *mll*.

DISCUSSION

Mll Morpholinos Generated a Defective Zebrafish Embryo Phenotype—In this study, we designed three morpholinos targeting zebrafish *mll.* In comparison with embryos injected with a standard control morpholino, *mll* morphants had defects in blood cell formation and altered *Hox* gene expression, consistent with defects seen in *MLL* null mice (17, 50). Because of the length of the zebrafish *mll* gene (4218 amino acids), we could not synthesize *mll* mRNA to perform rescue experiments; however, we observed that the *mll*-MO1, *mll*-MO2, and *mll*-MO3 morphants had very similar phenotypes, particularly in hematopoiesis, suggesting that the MO-mediated knockdown of *mll* is effective and specific.

In addition, we also showed that the N-terminal mini peptide (84 amino acids) might act as a dominant negative form of *mll* to disrupt the normal function of *mll* in hematopoiesis. The N terminus of MLL contains a highly conserved Menin-binding sequence at 5–10 amino acids, essential for MLL fusion protein-mediated leukemogenesis (44). To further determine whether zebrafish *menin* mediated the effect of N-terminal mini peptide, we designed and synthesized a morpholino to block translation (*menin*-MO, TCTTCTGAGTTGAACGAATCCCCAT) for zebrafish *menin* (Ensembl ID ENSDART00000080803). However, the *menin*-MO injected embryos did not display any detectable phenotypes, even with a very high dosage (24 ng/individual, data not shown). This result implies that *menin* probably was not responsible for the effect of N-terminal mini peptide. However, we could not rule out that other unidentified copies or homologs of *menin* played a redundant role. Given that the rearrangement of the *MLL* gene resulted in the N terminus fused with partner genes causes aggressive acute leukemias, the identification of a dominant negative domain of Mll in N-terminal might provide a useful clue for explaining the cause of leukemogenesis.

Zebrafish Primitive and Definitive Hematopoiesis Required mll—Zebrafish have two waves of hematopoiesis, primitive and definitive hematopoiesis (51). The series of genes that regulate hematopoiesis do so in a strictly controlled, time-dependent and spatially dependent manner. As revealed by the knock-out mouse models, *MLL* plays a major role in regulating mammalian hematopoiesis; however, the role that it plays in zebrafish hematopoiesis remains unknown, particularly during embryogenesis. In this study, we provide evidence to show that the knockdown of zebrafish *mll* affected both waves of zebrafish hematopoiesis. In the early embryonic stage, loss of *mll* resulted in reduced expression of the early hemangioblast markers *scl*

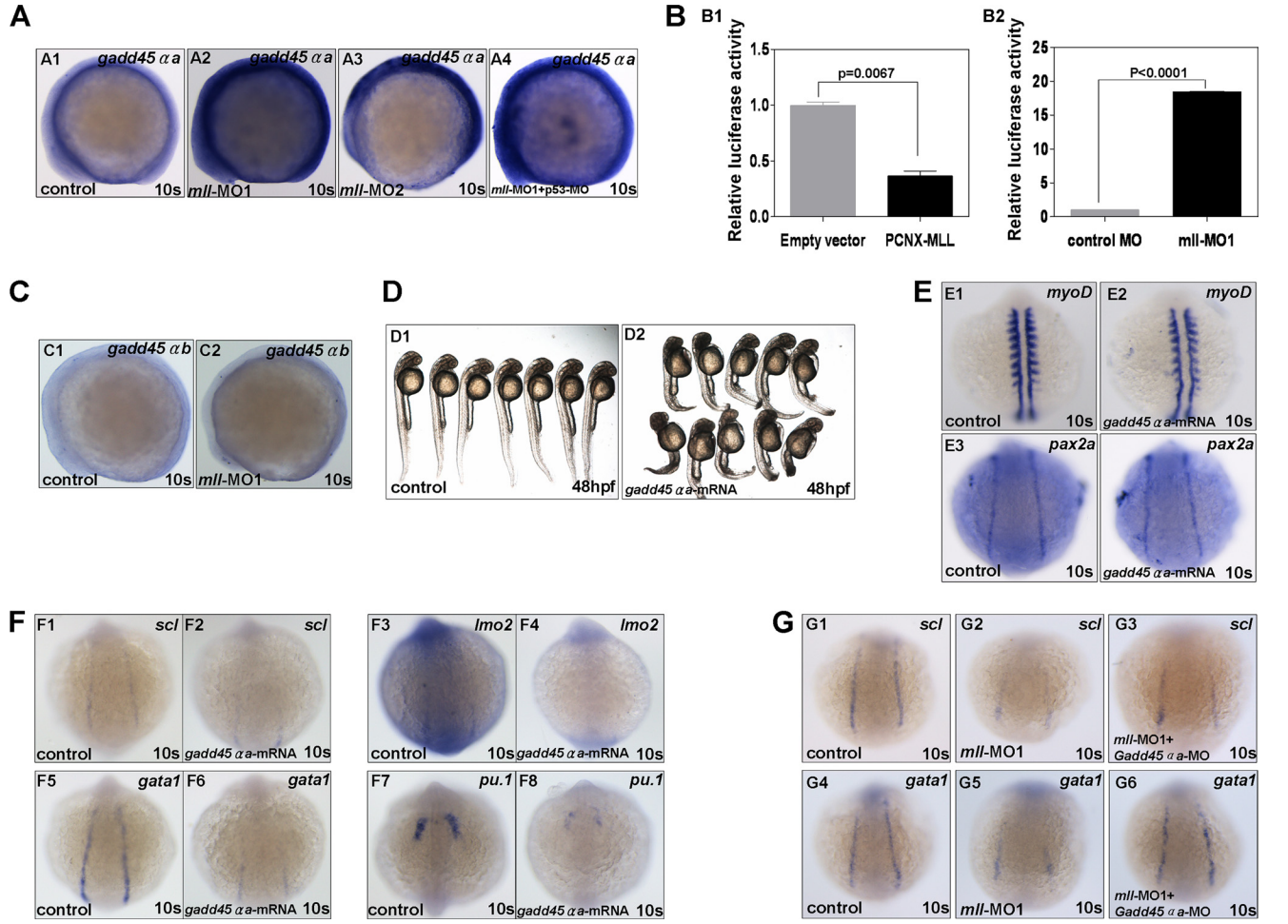

FIGURE 7. **Zebrafish *mll* effectively suppressed *gadd45αa* expression.** *A,* whole mount *in situ* hybridization assays for *gadd45αa* expression in embryos at 10-somite stage (lateral view). *Panel A1*, *gadd45αa* expression in embryos without *mll* morpholino injection (control); *panel A2*, *gadd45αa* expression in embryos injected with *mll*-MO1 (8 ng/per embryo); *panel A3*, *gadd45αa* expression in embryos injected with *mll*-MO2 (8 ng/per embryo); *panel A4*, *gadd45αa* expression in embryos injected with both *mll*-MO1 (8 ng/per embryo) and p53-MO(8 ng/per embryo). *B,* promoter luciferase reporter assays for *gadd45αa* regulation by either *mll* overexpression or *mll* knockdown in embryos. *Panel B1*, *gadd45αa* promoter activity was suppressed by human MLL overexpression significantly ($p < 0.05$); *panel B2*, *gadd45αa* promoter activity was enhanced by *mll* knockdown significantly ($p < 0.0001$). *C, gadd45αb* expression in embryos without *mll* morpholino injection (control) or injected with *mll*-MO1 (8 ng/per embryos) at 10-somite stage (lateral view). *Panel C1*, *gadd45αb* expression in embryos without *mll* morpholino injection (control); *panel C2*, *gadd45αa* expression in embryos injected with *mll*-MO1; *D,* morphology of embryos without mRNA injection (*control*) or injected with *gadd45αa* mRNA (400 ng/per embryo) at 48-hpf stage. *Panel D1*, control embryos; *panel D2*, embryos injected with *gadd45αa* mRNA. *E,* expression patterns of *myoD* and *pax2a* in embryos without mRNA injection (control) or injected with *gadd45αa* mRNA (400 pg/per embryo) at 10-somite stage. *Panels E1* and *E2*, *myoD*; *panel E3* and *E4*, *pax2a*. *F,* expression patterns of *scl*, *lmo2*, *gata1*, and *pu.1* in embryos without mRNA injection (*control*) or injected with *gadd45αa* mRNA (400 ng/per embryo) at 10-somite stage. *Panels F1* and *F2*, *scl*; *panels F3* and *F4*, *lmo2*; *panels F5* and *F6*, *gata1*; *panels F7* and *F8*, *pu.1*. *G, gadd45αa* mRNA (400 ng/per embryo) injection could partially rescue *scl* and *gata1* expression in *mll*-MO1 morphants. *Panels G1–G3*, *scl* rescued; *panels G4–G6*, *gata1* rescued.

and *lmo2,* as well as the erythroid progenitor marker *gata1* and the myeloid progenitor marker *pu1*. However, the pronephronic duct markers *pax2a* and precardiac marker *nkx2.5* were not affected. These results suggest that loss of *mll* specifically modulated hematopoiesis but not other mesoderm-derived tissues or organs. Besides the primitive hematopoietic markers, *mll* morphants also expressed reduced levels of definitive hematopoietic markers, including *runx1* and c-*myb.* Consequently, mature hematopoietic cell markers, such as *mpo*, *l-plastin*, and *hbbe1* were all significantly down-regulated. Blood flow tracing and hemoglobin staining demonstrated that *mll* depletion led to a severe disruption of mature blood cell formation.

Interestingly, 24-hpf *mll* morphants had a reduction in *gata1*-staining cells, and at 36 hpf, these *gata1*-staining cells still could be found in the intermediate cell mass. At this time point, *gata1*-marked cells should have developed into mature red blood cells. This phenomenon suggests that *mll* might contribute to controlling hematopoietic progenitor cell differentiation as well as their formation, consistent with its role in the mouse model. Regarding that the apoptosis induction by *mll* knockdown did not account for the effect of *mll* on hematopoiesis, that the cell proliferation was not affected by *mll* knockdown, and that *scl* and *lmo2* were reduced as early as the 5-somite stage in *mll* morphants, we think that *mll* might mainly modulate the formation and differentiation of hematopoietic progenitors. Recently, Robinson *et al.* (52) revealed that zebrafish *mll* expressed in hematopoietic tissue, also implying its role in hematopoiesis.

In Zebrafish, mll Regulated Hox Gene Expression, but Other mll Targets May Play Larger Roles in Hematopoiesis—As revealed by whole mount *in situ* hybridization, *mll* morphants had reduced expression levels of *hoxa9a*, *hoxb6b*, *hoxb4a,* and

hoxd3a, whereas microarray analysis showed a down-regulation of *hoxa10b, hoxa13a, hoxa2b,* and *hoxd3a*. These results suggest that zebrafish *mll* plays a critical role in maintaining expression of select *Hox* genes, similar to what occurs in mammals. However, none of the altered *Hox* genes could completely rescue the blood and morphology deficiency found in *mll* morphants, indicating that *Hox* genes may only be partially responsible for mediating the function of *mll* in hematopoiesis.

Gadd45αa Is a Potential Downstream Target of mll in Hematopoiesis Regulation—Through microarray analysis, we identified *gadd45αa* as being dramatically up-regulated in *mll* morphants. The results from whole mount *in situ* hybridization staining, promoter assays, and semi-quantitative RT-PCR further implicate *gadd45αa* as a direct target of *mll*; however, this will require confirmation through further assays such as chromatin immunoprecipitation and electrophoretic mobility shift assays (EMSA).

The embryos injected with synthesized *gadd45αa* phenotypically resembled the *mll* morphants, and co-injection of *gadd45αa*-MO could partially rescue the hematopoietic marker expression in *mll* morphants, suggesting a downstream role for *gadd45αa* in the regulation of hematopoiesis. However, *gadd45αa* overexpression could not alter *Hox* gene expression, and knockdown of *hoxa9a* and *hoxd3a* could not alter *gadd45αa* expression, which suggests that the regulation of *gadd45αa* by *mll* is parallel to that of *Hox* genes regulated by *mll*.

Of note, similar to *Hox* gene overexpression, *gadd45αa* knockdown could not rescue morphological phenotypes and blood flow in *mll* morphants, suggesting that multiple *mll* targets other than *Hox* genes and *gadd45αa* synergistically mediated the function of *mll* during embryogenesis. To further identify *mll*'s targets during embryogenesis will provide additional clues for understanding *mll*'s function both in morphogenesis and hematopoiesis.

Gadd45α, as a nonenzymatic factor, has been implicated in promoting demethylation (53). Although two studies (54, 55) questioned Gadd45α's function in promoting demethylation, a study using zebrafish embryos provided evidence to show that *gadd45* family members, including *gadd45α* (now named as *gadd45αb*), *gadd45αa*, *gadd45β,* and *gadd45γ,* participate in promoting 5-meC demethylation, implying an important role of *gadd45* in epigenetic regulation. Interestingly, we saw a connection between *gadd45αa* and *mll*, another epigenetic regulator. Determining the function of *gadd45αa* and *mll* in hematopoiesis will shed light on the underlying mechanisms regulating this important activity and provide a better understanding of how MLL fusion proteins induce leukemogenesis.

Acknowledgments—We gratefully acknowledge Drs. Stanley Kormeyers and Jianfang Gui for the generous gift of reagents.

REFERENCES

1. Ziemin-van der Poel, S., McCabe, N. R., Gill, H. J., Espinosa, R., 3rd, Patel, Y., Harden, A., Rubinelli, P., Smith, S. D., LeBeau, M. M., Rowley, J. D., and Diaz, M. O. (1991) *Proc. Natl. Acad. Sci. U.S.A.* **88,** 10735–10739
2. Djabali, M., Selleri, L., Parry, P., Bower, M., Young, B. D., and Evans, G. A. (1992) *Nat. Genet.* **2,** 113–118
3. McCabe, N. R., Burnett, R. C., Gill, H. J., Thirman, M. J., Mbangkollo, D., Kipiniak, M., van Melle, E., Ziemin-van der Poel, S., Rowley, J. D., and Diaz, M. O. (1992) *Proc. Natl. Acad. Sci. U.S.A.* **89,** 11794–11798
4. Gu, Y., Nakamura, T., Alder, H., Prasad, R., Canaani, O., Cimino, G., Croce, C. M., and Canaani, E. (1992) *Cell* **71,** 701–708
5. Tkachuk, D. C., Kohler, S., and Cleary, M. L. (1992) *Cell* **71,** 691–700
6. Hess, J. L. (2004) *Trends Mol. Med.* **10,** 500–507
7. Krivtsov, A. V., and Armstrong, S. A. (2007) *Nat. Rev. Cancer* **7,** 823–833
8. Marschalek, R. (2011) *Br. J. Haematol.* **152,** 141–154
9. Muntean, A. G., Giannola, D., Udager, A. M., and Hess, J. L. (2008) *Blood* **112,** 4690–4693
10. Milne, T. A., Briggs, S. D., Brock, H. W., Martin, M. E., Gibbs, D., Allis, C. D., and Hess, J. L. (2002) *Mol. Cell* **10,** 1107–1117
11. Liu, H., Takeda, S., Kumar, R., Westergard, T. D., Brown, E. J., Pandita, T. K., Cheng, E. H., and Hsieh, J. J. (2010) *Nature* **467,** 343–346
12. Hsieh, J. J., Ernst, P., Erdjument-Bromage, H., Tempst, P., and Korsmeyer, S. J. (2003) *Mol. Cell. Biol.* **23,** 186–194
13. Yokoyama, A., Kitabayashi, I., Ayton, P. M., Cleary, M. L., and Ohki, M. (2002) *Blood* **100,** 3710–3718
14. Yokoyama, A., Wang, Z., Wysocka, J., Sanyal, M., Aufiero, D. J., Kitabayashi, I., Herr, W., and Cleary, M. L. (2004) *Mol. Cell. Biol.* **24,** 5639–5649
15. Wysocka, J., Swigut, T., Milne, T. A., Dou, Y., Zhang, X., Burlingame, A. L., Roeder, R. G., Brivanlou, A. H., and Allis, C. D. (2005) *Cell* **121,** 859–872
16. Dou, Y., Milne, T. A., Tackett, A. J., Smith, E. R., Fukuda, A., Wysocka, J., Allis, C. D., Chait, B. T., Hess, J. L., and Roeder, R. G. (2005) *Cell* **121,** 873–885
17. Yu, B. D., Hess, J. L., Horning, S. E., Brown, G. A., and Korsmeyer, S. J. (1995) *Nature* **378,** 505–508
18. Yagi, H., Deguchi, K., Aono, A., Tani, Y., Kishimoto, T., and Komori, T. (1998) *Blood* **92,** 108–117
19. Ayton, P., Sneddon, S. F., Palmer, D. B., Rosewell, I. R., Owen, M. J., Young, B., Presley, R., and Subramanian, V. (2001) *Genesis* **30,** 201–212
20. Dobson, C. L., Warren, A. J., Pannell, R., Forster, A., and Rabbitts, T. H. (2000) *EMBO J.* **19,** 843–851
21. Terranova, R., Agherbi, H., Boned, A., Meresse, S., and Djabali, M. (2006) *Proc. Natl. Acad. Sci. U.S.A.* **103,** 6629–6634
22. Lim, D. A., Huang, Y. C., Swigut, T., Mirick, A. L., Garcia-Verdugo, J. M., Wysocka, J., Ernst, P., and Alvarez-Buylla, A. (2009) *Nature* **458,** 529–533
23. Hess, J. L., Yu, B. D., Li, B., Hanson, R., and Korsmeyer, S. J. (1997) *Blood* **90,** 1799–1806
24. Yamashita, M., Hirahara, K., Shinnakasu, R., Hosokawa, H., Norikane, S., Kimura, M. Y., Hasegawa, A., and Nakayama, T. (2006) *Immunity* **24,** 611–622
25. Yu, B. D., Hanson, R. D., Hess, J. L., Horning, S. E., and Korsmeyer, S. J. (1998) *Proc. Natl. Acad. Sci. U.S.A.* **95,** 10632–10636
26. Schilling, T. F., and Knight, R. D. (2001) *Philos. Trans. R. Soc. Lond. B Biol. Sci.* **356,** 1599–1613
27. Argiropoulos, B., and Humphries, R. K. (2007) *Oncogene* **26,** 6766–6776
28. Ernst, P., Mabon, M., Davidson, A. J., Zon, L. I., and Korsmeyer, S. J. (2004) *Curr. Biol.* **14,** 2063–2069
29. Magli, M. C., Barba, P., Celetti, A., De Vita, G., Cillo, C., and Boncinelli, E. (1991) *Proc. Natl. Acad. Sci. U.S.A.* **88,** 6348–6352
30. Krishnaraju, K., Hoffman, B., and Liebermann, D. A. (1997) *Blood* **90,** 1840–1849
31. Dorshkind, K., and Witte, O. (2004) *Mol. Cell* **13,** 765–766
32. McMahon, K. A., Hiew, S. Y., Hadjur, S., Veiga-Fernandes, H., Menzel, U., Price, A. J., Kioussis, D., Williams, O., and Brady, H. J. (2007) *Cell Stem Cell.* **1,** 338–345
33. Wan, X. Y., Ji, W., Mei, X., Zhou, J. G., Liu, J. X., Fang, C. C., and Xiao, W. H. (2010) *PLoS One* **5,** e91118
34. Thompson, M. A., Ransom, D. G., Pratt, S. J., MacLennan, H., Kieran, M. W., Detrich, H. W., 3rd, Vail, B., Huber, T. L., Paw, B., Brownlie, A. J., Oates, A. C., Fritz, A., Gates, M. A., Amores, A., Bahary, N., Talbot, W. S., Her, H., Beier, D. R., Postlethwait, J. H., and Zon, L. I. (1998) *Dev. Biol.* **197,** 248–269
35. Krauss, S., Johansen, T., Korzh, V., and Fjose, A. (1991) *Nature* **353,** 267–270

36. Tu, C. T., Yang, T. C., and Tsai, H. J. (2009) *Plos One* **4,** e4249
37. Zhong, T. P., Childs, S., Leu, J. P., and Fishman, M. C. (2001) *Nature* **414,** 216–220
38. Rai, K., Huggins, I. J., James, S. R., Karpf, A. R., Jones, D. A., and Cairns, B. R. (2008) *Cell* **135,** 1201–1212
39. Yang, Z., Liu, N., and Lin, S. (2001) *Dev. Biol.* **231,** 138–148
40. Zhou, J., Feng, X., Ban, B., Liu, J., Wang, Z., and Xiao, W. (2009) *J. Biol. Chem.* **284,** 19142–19152
41. Lee, P., Goishi, K., Davidson, A. J., Mannix, R., Zon, L., and Klagsbrun, M. (2002) *Proc. Natl. Acad. Sci. U.S.A.* **99,** 10470–10475
42. Mende, M., Christophorou, N. A., and Streit, A. (2008) *Mech. Dev.* **125,** 947–962
43. Tittle, R. K., Sze, R., Ng, A., Nuckels, R. J., Swartz, M. E., Anderson, R. M., Bosch, J., Stainier, D. Y., Eberhart, J. K., and Gross, J. M. (2011) *Dev. Biol.* **350,** 50–63
44. Yokoyama, A., Somervaille, T. C., Smith, K. S., Rozenblatt-Rosen, O., Meyerson, M., and Cleary, M. L. (2005) *Cell* **123,** 207–218
45. Davidson, A. J., Ernst, P., Wang, Y., Dekens, M. P., Kingsley, P. D., Palis, J., Korsmeyer, S. J., Daley, G. Q., and Zon, L. I. (2003) *Nature* **425,** 300–306
46. Diehl, F., Rössig, L., Zeiher, A. M., Dimmeler, S., and Urbich, C. (2007) *Blood* **109,** 1472–1478
47. Kyba, M., Perlingeiro, R. C., and Daley, G. Q. (2002) *Cell* **109,** 29–37
48. Antonchuk, J., Sauvageau, G., and Humphries, R. K. (2002) *Cell* **109,** 39–45
49. Rosemary Siafakas, A., and Richardson, D. R. (2009) *Int. J. Biochem. Cell Biol.* **41,** 986–989
50. Lim, D. A., Huang, Y. C., Swigut, T., Mirick, A. L., Garcia-Verdugo, J. M., Wysocka, J., Ernst, P., and Alvarez-Buylla, A. (2009) *Nature* **458,** 529-U533
51. de Jong, J. L., and Zon, L. I. (2005) *Annu. Rev. Genet.* **39,** 481–501
52. Robinson, B. W., Germano, G., Song, Y., Abrams, J., Scott, M., Guariento, I., Tiso, N., Argenton, F., Basso, G., Rhodes, J., Kanki, J. P., Look, A. T., Balice-Gordon, R. J., and Felix, C. A. (2011) *Br. J. Haematol.* **152,** 307–321
53. Barreto, G., Schäfer, A., Marhold, J., Stach, D., Swaminathan, S. K., Handa, V., Döderlein, G., Maltry, N., Wu, W., Lyko, F., and Niehrs, C. (2007) *Nature* **445,** 671–675
54. Jin, S. G., Guo, C., and Pfeifer, G. P. (2008) *PloS Genet.* **4,** e1000013
55. Engel, N., Tront, J. S., Erinle, T., Nguyen, N., Latham, K. E., Sapienza, C., Hoffman, B., and Liebermann, D. A. (2009) *Epigenetics* **4,** 98–99